An Integrated Protective Scheme for a multi- ended Egyptian Transmission Line using Radial Basis Neural Network

El Sayed Tag Eldin, *Senior Member, IEEE,* Hany Elghazaly, *Senior Member, IEEE,* Mohamed Moussa

Abstract -- This paper presents a novel approach to fault detection, faulty phase(s) identification, faulty section estimation, and fault location determination for a multi-ended transmission line in Egypt based on artificial neural networks. In order to perform this approach, the protection task is subdivided into different neural network modules for fault detection, fault classification as well as fault location. The suggested approach uses the Radial Basis Function Artificial Neural Network (RBFANN). The proposed scheme consists of nine RBFANNs, one for fault classification and faulty phase identification, four networks for faulty section estimation one for each fault type, and four networks for fault location within the faulty section, again one for each fault type. The three-phase voltages and currents are sampled at 1 kHz. Pre and post-fault data are utilized as inputs for the proposed scheme. The Electromagnetic Transient Program (EMTP) is used to generate simulation data for the typical Egyptian 500 kV transmission line in normal and faulty conditions to train and test the RBFNN. Testing results proved that the proposed RBF networks could provide great performance for high speed relaying. It is accurate, fast, and reliable.

Keywords: Digital protection, Artificial neural networks, Egypt network, Radial Basis Function, Transmission line.

I. INTRODUCTION

POWER system protection is a vital prerequisite for the efficient operation and continuing development of power systems [1]. Transmission lines are the connecting links between the generation stations and the distribution systems, and lead to other power system networks over interconnections. Fast and accurate location of the faults in an electrical power transmission line is vital for the secure and economic operation of power systems. This is more so in view of the fact that as a result of an increase in transmission requirements and environmental pressures, utilities are being forced to maximize the transmission line capabilities of the existing transmission lines. This effectively means that in order to maintain system security and stability, there is a demand for minimizing damage by restoring the faulty line as quickly as possible. Thus, the protective system shall be reliable, selective and very sensitive to all types of faults.

Recently artificial neural network (ANN) has gained a good success in many power applications [2-14]. Many advantages are inherent in ANNs, including the excellent noise immunity and robustness, making their use less susceptible to operating conditions than conventional approaches. The typical Back-Propagation Neural Network (BPNN) has been used for transmission line protection [2-9]. BPNN is a nonlinear regression technique which attempts to minimize the global error. Its training process includes the forward and backward propagation, with the desired output used to generate error values for back propagation to iteratively improve the output. However, despite its wide applications, BP has a number of deficiencies, such as slow training and local minimum and is not well suited for transmission-line relaying, as the algorithm does not work satisfactorily when the case to be diagnosed falls in a region with no training data. The radial-basis-function (RBF) based neural network is well suited for such cases [10-14].

The RBF neural network is different from BP with sigmoidal activation functions utilizing basis functions in the hidden layer, which are locally responsive to input stimulus. These hidden nodes are usually implemented with a Gaussian kernel. Each hidden node in an RBF neural network has a radial symmetrical response around the center vector, and the output layer is a set of linear weighted combiners. However, performance of the RBF neural network critically depends upon the chosen centers, which is not suitable for sequential learning and may require an unnecessarily large RBF network to obtain a given level of accuracy and cause numerical ill-conditioning. These shortcomings can be overcome by reformulating the learning problem. In this paper minimal RBF neural network (MRBFNN), where the learning process is sequential, is used. The network starts with no hidden unit and hidden units are added based on novelty of the data. A new pattern is considered novel if the input is far away from the existing centre, error between the desired output and network output is large and the rms error is also significant. If the data set does not satisfy the above criteria no hidden neuron is added. Radial basis function neural networks (RBFNNs) are suitable for solving pattern classification problems due to their simple topological structure and their ability to reveal how learning proceeds in an explicit manner [13,14].

This paper presents a non-communication technique for the protection of multi terminal transmission line. It presents the fault classification and location algorithm using MRBFNN. An intelligent learning procedure is used. It constructs a compact RBF networks in a rational way, preserving the advantages of linear learning. In this strategy

E.M. Tag Eldin is an Assistant Professor and H.A. Elghzaly is a Professor at Cairo University, Faculty of Engineering, Electric Power and Machines Department, Giza, Cairo **(stageldin@ieee.org).**

M.A. Moussa is a Control Engineer in the Cairo Electric Power Distribution Company.

Presented at the International Conference on Power Systems Transients (IPST'05) in Montreal, Canada on June 19-23, 2005
Paper No. IPST05 - 165

the network starts with no hidden unit and hidden units are added based on the novelty of the data [11-12]. The main objectives of this paper are: Firstly, realizing the powerful and robustness of MRBFNN for classifying different states of operation for transmission system including normal operation, single line to ground fault, double line fault, double line to ground fault and three lines to ground fault, secondly, detecting the faulty section in case of fault occurrence, thirdly, accurately allocating the fault within the faulty section. In this paper only one neural network is capable to achieve both, fault classification and faulty phase identification. Four neural networks are used for faulty section estimation one for each fault type, and other four networks are used for accurate fault location within the faulty section, again one for each type.

Existing Egyptian multi-ended 500 kV transmission line is used as a real application to show the validity of the proposed algorithm. The system is simulated using Electromagnetic transient program EMTP and the neural networks are trained using the simulation measurements consisting of three-phase-sampled voltages at CAIRO500 bus and currents at the two circuits, KURAIMAT – CAIRO500, and SAMALUT – CAIRO500 at the same bus at a sampling rate of 1 kHz.

Finally, the designed relay is tested using simulated fault patterns not presented during the training process.

II. Neural Networks Overview

ANN technology is a branch of artificial intelligence involving fuzzy logic and genetic algorithms. The drawback of the popular types of the ANNs is the need for a lot of trials to get the optimum structure with the optimum number of hidden layers and neurons. In this paper the Minimum Radial Basis Function Neural Network is used.

The RBF network structure model consists of three layers, the input layer, the hidden layer, and the output layer. The nodes within each layer are fully connected to the previous layer. The input variables are assigned to each node in the input layer and are passed directly to the hidden layer without weights. The hidden nodes (neurons) contain the radial basis functions. Any of the functions, namely spline, multi-quadratic and Gaussian function, may be used as a transfer function for the hidden neurons. The Gaussian RBF, which is the most widely used, has been considered for the proposed fault classification and location applications.

The response $a_i(x_p)$ of the ith unit in the hidden layer to the network input x_p is given by

$$a_i(x_p) = \exp\left(-\frac{\|x_p - \mu_i\|^2}{\sigma_i^2}\right) \quad (1)$$

Where μ_i is the center vector for the hidden unit, σ_i is the width of the Gaussian function, and $\|\ \|$ denotes the Euclidean norm.

The connection between the hidden units and the output units are weighted sums. The output value o_{qp} of the qth output node is given as

$$o_{qp} = w_{qo} + \sum_{i=1}^{H} w_{qi}\, a_i(X_p) \quad (2)$$

Where H indicates the total number of hidden neurons in the network, w_{qi} is the connecting weight of the ith hidden unit to the qth output node and w_{qo} is the bias term for the corresponding qth output neuron.

The learning process of the MRBFNN involves the allocation of new hidden units and the tuning of network parameters. The network structure starts with no hidden units at first and as training continues more additional hidden units are added to the structure depending on the novelty in the data. A new pattern is considered novel if the input is far away from the existing centre, the error between the desired output and network output is large and the rms error is significant. If the data set does not satisfy the above criteria, no hidden neuron is added. This particular architecture of RBFNN has proved to directly improve training and performance of the network [10-12].

During training of the RBF network, care has been taken to avoid network memorization or over training. When a neural network memorizes the training data, it produces acceptable results for patterns used for training but provides incorrect output when tested on unseen data. To ensure that the neural network has learned and not memorized by reshuffling of the training patterns was performed to get almost equal errors during training and testing. It was observed that the training error decreases along with number of iterations, while the testing error decreases at first, bounces around, and then starts increasing. The optimal learning is achieved at the global minimum of testing error.

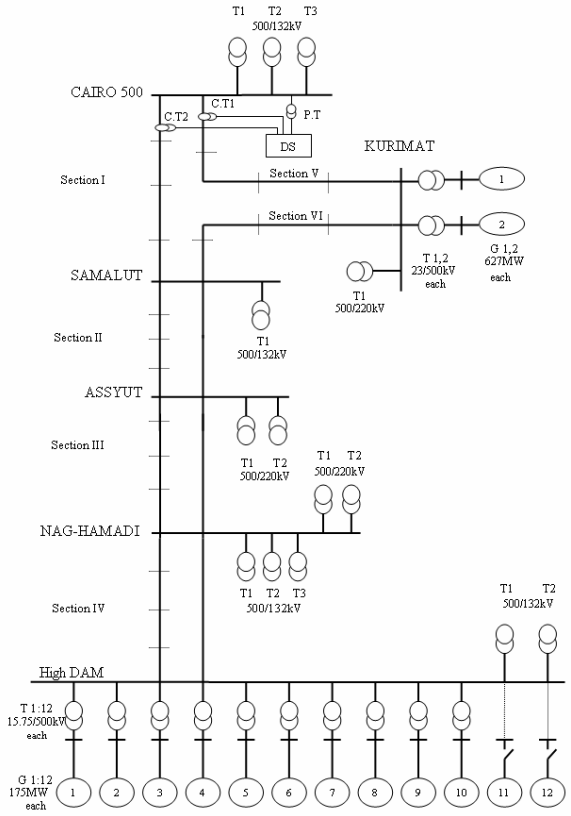

Fig. 1 Single line diagram of the system under study.

III. System under Study

The strategic part of the Egyptian unified power system is used as a real application to train and test the suggested algorithm. The existing Upper Egypt power system shown in figure 1 consists of HIGH DAM–CAIRO500, HIGH DAM–KURAIMAT and KURAIMAT–CAIRO500 transmission lines. It contains the largest power generation station in Egypt which is HIGH DAM power generation station. It contains also the largest steam power generation station in the Middle East which is KURAIMAT power generation station.

A. Circuit Representation

1) Transmission Circuits:

The system consists of three transmission circuits:

a) HIGH DAM – CAIRO500:

This circuit is a single circuit line of a length 789km beginning at HIGH DAM station and ending at CAIRO500 station. The line passes also through NAG HAMADI, ASSIUT, and SAMALUT.

b) HIGH DAM – KURAIMAT:

This circuit is a single circuit line of a length 734km beginning at HIGH DAM station and ending at KURAIMAT station. The line passes through NAG HAMADI, ASSIUT, and SAMALUT.

c) KURAIMAT – CAIRO500:

This circuit is a single circuit line of a length 125km beginning at KURAIMAT station and ending at CAIRO500 station.

2) Generation stations:

a) HIGH DAM:

It includes twelve generation units each of 175 MW, ten of them are in operation, and twelve transformer units 15.75/500 kV each of 206 MVA, ten of them are in operation.

b) KURAIMAT:

It includes two generation units each of 627 MW and two Transformer units 23/500 kV each of 812 MVA.

3) Transformer stations:

a) HIGH DAM:

It contains two transformers 500/132 kV, 375MVA each.

b) NAG HAMADI:

It contains two transformers 500/220 kV, 375 MVA each and three transformers 500/132 kV, 285MVA each.

c) ASSIUT:

It contains two transformers 500/132 kV, 375 MVA each.

d) SAMALUT:

It contains one transformer 500/132 kV of 285 MVA.

e) KURAIMAT:

It contains one transformer 500/220kV of 285 MVA.

f) CAIRO500:

It contains three transformers 500/ 132kV, 285 MVA each.

B. Load Centers:

The power system under consideration is a heavily loaded power system as it contains the most important industrial loads such as Nag Hammady Aluminum factory, Ferrosilicon, Kima, and cement factories. The load distribution at different station buses is listed in table I.

TABLE I
LOADS AT DIFFERENT STATIONS IN THE SYSTEM UNDER STUDY

Station Bus	Load (MW and MVAR)
HIGH DAM	364.7+J208.8
NAG HAMMADI	799.3+j481.7
ASSIUT	232.2+j114.4
SAMALUT	167.9+j147.7
KURAIMAT	173.2+j 97.9
CAIRO 500	392.4+j650.1

IV. System simulation

Due to limited available amount of practical fault data, it is necessary to generate examples of fault waveforms using simulation. To generate data for the typical transmission system, digital simulations were performed for different faults using EMTP which was used to generate three voltages and six current signals samples at CAIRO500 terminal of the system shown in figure 1. The simulation of different fault types (a-g, b-g, c-g, a-b, b-c, c-a, ab-g, bc-g, ca-g, and abc-g) and conditions (inception angles 0º, 54º, 90º, and fault resistances 0Ω, 100Ω) were conducted at various locations on the transmission lines. The sampled data represents the system characteristics. Therefore, the sampling rate 1 kHz, corresponding to 20 samples per cycle on a 50 Hz base was selected in this paper. This provides a well convergence performance. Despite the parallel processing capability of ANN, for further decrease in the computation time, the input vector dimension is decreased by reducing the number of samples in a data window. A four sampled data window is collected for each signal to converge to the required value.

V. Design of minimal radial basis function neural network

The proposed scheme can achieve protective relaying tasks including fault detection and classification, faulty-section discrimination, as well as fault location. The algorithm starts by collecting the sampled data. The design of the MRBF algorithm is realized in two stages, the first stage being a pre-processing stage, and the second stage being feature extraction using MRBFNNs.

A. Pre-processing

The Pre-processing stage algorithm consists of two steps, namely filtering and normalization.

1) Filtering

The post-fault voltage and current signals are corrupted by high frequency transients, which may not be suitable for the learning of the proposed algorithm. The nine signals are filtered using a zero phase digital filter to attenuate the DC and high frequency transient components.

2) Normalization

The voltage and current signals were normalized. The normalized voltage and current values are clipped to -1 and +1 if they are outside the interval [-1, +1].

B. Feature Extraction using MRBFNN

The second stage contains nine networks, one for fault classification as well as faulty phase identification, four

networks for faulty section estimation, and other four networks for accurate fault location within the faulty section.

1) Fault Detection and Classification

A single RBF network is obtained for the three purposes, fault detection, fault classification and faulty phase identification. The input layer contains 36 inputs corresponding to nine input variables, three voltages and six currents, each with 4 samples in a data-window. A hidden layer of 700 neurons is selected. The transfer function used for the hidden layer neurons is Gaussian. The output layer contains four neurons. The outputs contain variables whose values are given 0 or 1 relating to three phases (A, B, C) and the ground (G). This can be extended to represent all practical fault types for all three transmission circuits shown in figure 1 involving the various combinations of phases at different operating system conditions.

2) Faulty Section Estimation

The system under study is subdivided into six sections as shown in figure 1. Four MRBFNN are designed each network capable to estimate faulty section, one for each fault type. The first NN for single line to ground, the second for double line fault, the third for double line to ground fault, and the fourth for three line to ground fault. The samples of the three phase voltages at CAIRO500 bus and currents in SAMALUT circuit at CAIRO500 bus are used to train and build the neural network knowledge base to get output dependent on the faulty section. The input layer contains 24 inputs corresponding to six input variables three voltages and three currents, each with four samples in a data-window. A hidden layer of 50 neurons is selected. The output layer contains one output neuron corresponding to the faulty section. The transfer function used for the hidden layer neurons is Gaussian.

3) Fault Location

To estimate the exact fault location within the faulty section other four MRBF neural networks (again one for each fault type) are trained with the voltages and currents as in faulty section estimation, while the output is the fault location as per unit of the section length. The structure of the proposed fault locator is similar to that of the faulty section estimator, where the input layer contains the same 24 inputs. The hidden layer contains 50 neurons and the output layer contains one output neuron corresponding to the fault location. The transfer function used for the hidden layer neurons is Gaussian.

VI. Test Results And Discussion

A. Fault Classification MRBFNNs

Different fault types at various locations of each section of the system under study with different inception angles and fault resistance (which were not used in the training stage) were used to test the RBFNN. During the process of calculation, the "one" and "zero" outputs of the NN are formed within a tolerance 0.002%. This means that when the output is near zero, it is taken as zero and when the output is near one, it is taken as one. The RMS error convergence diagram is shown in figure 2.

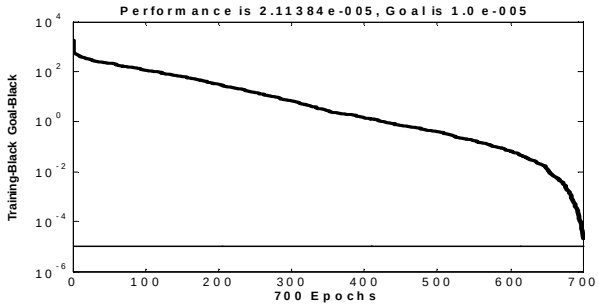

Fig. 2 RMS error convergence diagram for the fault classification RBFNN as a function of the number of epochs

Table II shows some of the test results for different system conditions and not presented to the neural network during the training process. For each case it can be seen that the values of (A, B, C and G) converge to the required values, and are either very close to zero or to one.

TABLE II
TESTING RESULTS OF THE RBF NETWORK FOR FAULT CLASSIFICATION AND FAULTY PHASE IDENTIFICATION (NN1)

case	Fault Inception	Fault Resistance	Faulty Section	Result output			
				A	B	C	G
n	n	n	n	-0.0000	-0.0000	0.0000	0.0000
a-g	54	0	1	1.0207	0.0188	0.0270	1.0275
a-g	0	100	4	0.9646	-0.0026	0.0131	0.9957
b-g	90	100	3	-0.0103	1.0281	0.0318	0.9813
c-g	0	0	4	0.0825	-0.0202	0.9988	1.0572
a-b	0	0	2	0.9845	1.0141	0.0072	0.0032
b-c	54	0	5	-0.0323	0.9793	1.0405	-0.0585
c-a	54	0	4	0.9986	0.0118	0.9974	-0.0154
ab-g	54	0	6	1.0554	0.8705	-0.0329	1.1097
bc-g	54	0	2	-0.0899	1.0508	0.9319	0.9192
ca-g	0	0	6	1.2345	-0.2098	0.9470	1.1821
abc-g	90	100	4	1.2484	0.8527	1.0343	1.1475

B. Faulty Section Estimation MRBFNNs

All types of faults with different inception angles and different locations of each section of the HIGHDAM-CAIRO500 circuit of the system under study were simulated to get the training and the testing data for MRBFNNs. Each network was trained and tested with patterns at 25, 50% and 75% of each section. During the training process, the output digit of the ANN is formed within a tolerance of 0.01%. The RMS error convergence diagram is shown in figure 3.

Random selected testing results for different fault types (which were not presented to the neural networks during the training process) are shown in tables III, IV, V and VI.

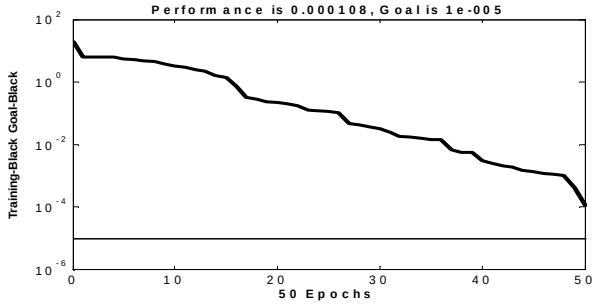

Fig. 3 RMS error convergence diagram for faulty section estimation RBFNN as a function of the number of epochs

TABLE III
TESTING RESULTS OF THE MINIMAL RBF NETWORK FOR SINGLE LINE TO GROUND FAULT (NN2)

Fault Type	Fault Inception Angle (Θº)	Faulty Section	Target	Result Output
a-g	54	SAM-CA	1	1.1076
b-g	90	SAM-CA	1	0.6391
c-g	0	SAM-CA	1	0.6201
a-g	90	AS-SAM	2	2.2392
b-g	54	AS-SAM	2	2.1587
b-g	90	AS-SAM	2	2.1181
b-g	90	NH-AS	3	3.1178
c-g	0	NH-AS	3	3.1769
c-g	54	NH-AS	3	2.9251
a-g	54	HD-NH	4	4.0585
a-g	90	HD-NH	4	4.1496
b-g	0	HD-NH	4	4.0594

TABLE IV
TESTING RESULTS OF THE MINIMAL RBF NETWORK FOR DOUBLE LINE FAULT (NN3)

Fault Type	Fault Inception Angle (Θº)	Faulty Section	Target	Result Output
a-b	0	SAM-CA	1	0.8065
b-c	54	SAM-CA	1	1.1092
b-c	90	SAM-CA	1	1.1942
a-b	54	AS-SAM	2	2.1088
b-c	0	AS-SAM	2	2.1114
c-a	0	AS-SAM	2	2.0339
b-c	54	NH-AS	3	2.8823
b-c	90	NH-AS	3	3.2342
c-a	0	NH-AS	3	3.0147
a-b	54	HD-NH	4	4.0103
b-c	54	HD-NH	4	4.1363
c-a	0	HD-NH	4	4.0124

TABLE V
TESTING RESULTS OF THE MINIMAL RBF NETWORK FOR DOUBLE LINE TO GROUND FAULT (NN4)

Fault Type	Fault Inception Angle (Θº)	Faulty Section	Target	Result Output
ab-g	0	SAM-CA	1	0.9999
ab-g	54	SAM-CA	1	1.0191
ca-g	90	SAM-CA	1	1.0606
ab-g	0	AS-SAM	2	2.0172
bc-g	90	AS-SAM	2	2.1242
ca-g	54	AS-SAM	2	2.1638
bc-g	54	NH-AS	3	3.0617
bc-g	90	NH-AS	3	3.0999
ca-g	0	NH-AS	3	3.1411
ab-g	0	HD-NH	4	4.2089
bc-g	54	HD-NH	4	4.0722
ca-g	0	HD-NH	4	4.0674

TABLE VI
TESTING RESULTS OF THE MINIMAL RBF NETWORK FOR THREE LINE TO GROUND FAULT (NN5)

Fault Type	Fault Inception Angle (Θº)	Faulty Section	Target	Result Output
abc-g	54	SAM-CA	1	1.0581
abc-g	54	AS-SAM	2	2.3874
abc-g	90	NH-AS	3	3.1757
abc-g	0	HD-NH	4	4.2566

C. Accurate Fault Location MRBFNNs

All types of faults with different inception angles and different locations at (0, 10, 20, 30… 100%) of SAMALUT-CAIRO500 section from the circuit under study were simulated to get the training and testing patterns for the MRBFNNs. During the testing process, the output digit of the ANN is formed within a tolerance 0.003%. The RMS error convergence diagram is shown in figure 4.

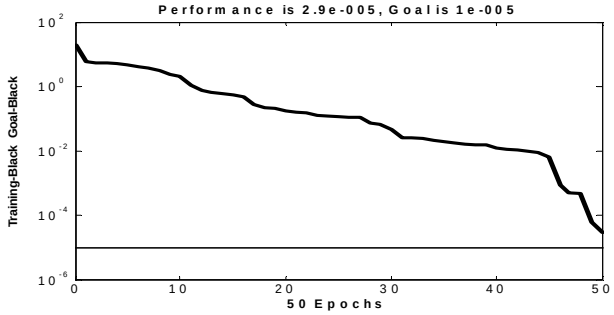

Fig. 4 RMS error convergence diagram for fault location RBFNN as a function of the number of epochs

Selective testing results for different fault types (which were not presented to the neural networks during the training process) are shown in tables VII, VIII, IX and X.
The error is calculated by:

$$\% \text{ Error } = \frac{\left|\text{Actual fault location } - \text{Calculated fault location}\right|}{\text{Total faulty section length}} * 100 \quad (3)$$

TABLE VII
TESTING RESULTS OF THE MINMAL RBF NETWORK FOR SINGLE LINE TO GROUND FAULT (NN6)

Fault type	Fault Inception Angle (θº)	Actual Fault Location	Estimated Fault Location	%Error
a-g	0	0.30	0.3009	0.09
a-g	54	0.30	0.3065	0.65
a-g	0	0.50	0.4983	0.17
a-g	0	0.70	0.7017	0.17
b-g	54	0.30	0.2868	1.32
b-g	54	0.50	0.5103	1.03
b-g	90	0.90	0.8894	1.06
c-g	54	0.10	0.1004	0.04
c-g	54	0.30	0.2986	0.14
c-g	54	0.50	0.4967	0.33
c-g	90	0.50	0.5058	0.58

TABLE VIII
TESTING RESULTS OF THE MINMAL RBF NETWORK FOR DOUBLE LINE TO GROUND FAULT (NN7)

Fault type	Fault inception angle(θº)	Actual Fault location	Estimated Fault Location	% Error
a-b	0	0.10	0.1060	0.6
a-b	0	0.50	0.5149	1.49
a-b	54	0.50	0.5010	0.1
a-b	54	0.70	0.6854	1.46
b-c	90	0.30	0.3046	0.46
b-c	90	0.50	0.5028	0.28
b-c	54	0.70	0.7130	1.3
b-c	90	0.70	0.6967	0.33
b-c	0	0.90	0.9110	1.1
c-a	54	0.50	0.5109	1.09

TABLE IX
TESTING RESULTS OF THE MINMAL RBF NETWORK FOR DOUBLE LINE TO GROUND FAULT (NN8)

Fault type	Fault inception angle(θ^o)	Actual Fault location	Estimated Fault Location	% Error
ab-g	54	0.10	0.1176	1.76
ab-g	0	0.50	0.5153	1.53
ab-g	90	0.50	0.4952	0.48
ab-g	90	0.70	0.7094	0.94
bc-g	54	0.30	0.3025	0.25
bc-g	90	0.30	0.2994	0.06
bc-g	54	0.50	0.5013	0.13
bc-g	90	0.50	0.5081	0.81
bc-g	90	0.70	0.7078	0.78
ca-g	54	0.30	0.3212	2.12

TABLE X
TESTING RESULTS OF THE MINIMAL RBF NETWORK FOR THREE LINE TO GROUND FAULT (NN9)

Fault Type	Fault Inception Angle (Θ^o)	Actual Fault location	Estimated Fault Location	% Error
abc-g	54	0.30	0.3250	2.5
abc-g	90	0.90	0.9160	1.6
abc-g	0	0.50	0.5132	1.32
abc-g	90	0.70	0.6729	2.71

VII. CONCLUSIONS

In this paper, a novel integrated protective scheme for EHV multi-ended transmission system is introduced. A new structure of neural network diagnostic system for fault classification, faulty phase identification, faulty section estimation, and reasonably accurate fault location is proposed. The technique is based on the use of the Radial Basis Function Artificial Neural Network. The proposed scheme deals with all types of faults and all fault conditions, including different fault types, fault inception angles, fault resistance, and fault location. As a case study, the Upper Egypt 500kV transmission system was established by collecting elemental samples of voltage and current waveforms using EMTP. The diagnosis system consists of two hierarchical levels. The first is for pre-processing and the second for neural networks. These networks are responsible for fault classification as well as faulty phase identification, faulty section estimation and fault location within the faulty section. The new structure of the RBFANN can be easily adapted to deal with the changes of relaying scheme through the user interface. Accuracy in testing results was reasonable, irrespective of different system conditions. Therefore, it validates the proposed Diagnosis system for cases contained in the training set as well as for new testing cases.

VIII. REFERENCES

[1] S.H. Horowitz. A.G. Phadke. Power System Relaying. Wiley, 1995.

[2] D. V. Coury and D. C. Jorge, “Artificial Neural Network Approach to Distance Protection of Transmission Lines,” *IEEE Trans. on Power Delivery*, vol. 13, pp. 102–108, Jan. 1998.

[3] H.Wang andW.W. L. Keerthipala, “Fuzzy-Neuro Approach to Fault Classification for Transmission Line Protection,” *IEEE Trans. on Power Delivery*, vol. 13, pp. 1093–1102, Oct. 1998.

[4] T.S. Sidhu, H. Singh, and M.S. Sachdev, "Design Implementation and Testing of An Artificial Neural Network Based Fault Direction Discriminator for Protecting Transmission Lines," *IEEE Trans. on Power Delivery*, vol. 10, no. 2, pp. 697-706, Apr. 1995.

[5] T. Dalstein and B. Kulicke, “Neural network Approach to Fault Classification for High Speed Protective Relaying,” *IEEE Trans. on Power Delivery*, vol. 10, no. 2, pp. 1002–1009, Apr. 1995.

[6] T. Dalstein, T. Friedrich, B. Kulicke, and D. Sobajic, "Multi Neural-Network Based Fault Area Estimation for High Speed Protective Relaying," *IEEE/PES Summer Power Meeting*, Portland, July 1995, Paper Number 95 SM 431-7 PWRD.

[7] A. F. Sultan, G. W. Swift, and D. J. Federchuk, "Detection of High Impedance Arcing Faults Using a Multi Layer Perceptron," *IEEE Trans. on Power Delivery*, vol. 7, no.4, pp. 1871-1877, Oct. 1992.

[8] R. K. Aggarwal, Q. Y. Xuan, R. W. Dunn, A. T. Johns, and A. Bennett, “Novel Fault Classification Technique for Double-Circuit Lines Based on a Combined Unsupervised/Supervised Neural Network,” *IEEE Trans. on Power Delivery*, vol. 14, no. 4, pp. 1250-1255, Oct. 1999.

[9] L. Ángel, F. Fernandez, and N.K. Ghonaim "Novel Approach Using a FIRANN for Fault Detection and Direction Estimation for High-Voltage Transmission Lines." *IEEE Trans. on power delivery*, Vol. 17, No. 4, pp. 894-900, oct. 2002.

[10] S. Chen. C. F. N. Cowan, and P.M. Grant, "Orthogonal Least Squares Learning Algorithm for Radial Basis Function Networks," *IEEE Trans. on Neural Network*, vol. 2, no. 2, pp. 302-309, Mar. 1991.

[11] L. Yingwei, N. Sundarrajan, and P. Saratchandran, "Performance Evaluation of a Sequential Minimal Radial Basis Function (RBF) Neural Network Learning Algorithm," *IEEE Trans. on Neural Networks*, vol. 9, no. 2, pp. 308-318, 1998.

[12] E.M. Tageldin, M.M. El Khairy, H.M.Elghazaly, “Application of the Minimal Radial Basis Neural Network to Fault Classification and Faulty Phase Identification on Egyptian 500 kV Transmission System" Seventh Middle East Power System Conference MEPCON, pp.537-543, Egypt, 2003.

[13] K. G. Narendra, V. K. Sood, K. Khorasani, and R. Patel, "Application of a Radial Basis Function (RBF) Neural Network for Fault Diagnosis in HVDC Systems," *IEEE Trans. on Power Systems*, vol. 13, no. 1, pp. 177-183, 1998.

[14] R.N. Mahanty and P.B. Dutta Gupta “Application of RBF neural network to fault classification and location in transmission lines ,“ IEE Proceedings on Generation Transmission and Distribution., Vol. 151, No. 2, pp. 201-212, March 2004.